SUPPLEMENTARY INFORMATION

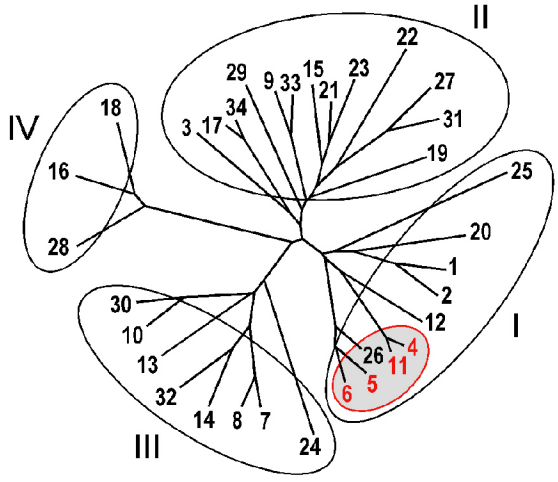

Supplementary Figure 1 | Relation tree of Arabidopsis CPKs. The complete protein sequences were aligned and analyzed with ClustalX and Treeview algorithms. The *CPK* genes in subgroup I involved in flg22 signalling are highlighted.

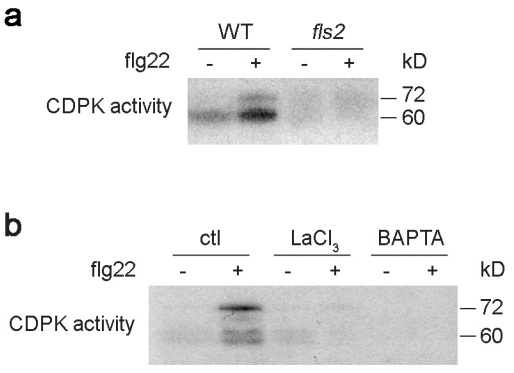

Supplementary Figure 2 | Flg22 activation of endogenous CDPKs requires FLS2 and calcium signalling. Endogenous CDPK activity was analyzed in protoplasts using an in-gel kinase assay with histone as an artificial substrate. **a,** Protoplasts from WT (Ler) or *fls2* mutant were treated with 100 nM flg22 for 20 min. **b,** Protoplasts from WT (Col-0) were treated with 2 mM $LaCl_3$, 4 mM BAPTA or H_2O control (ctl) for 15 min prior to elicitation with 100 nM flg22.

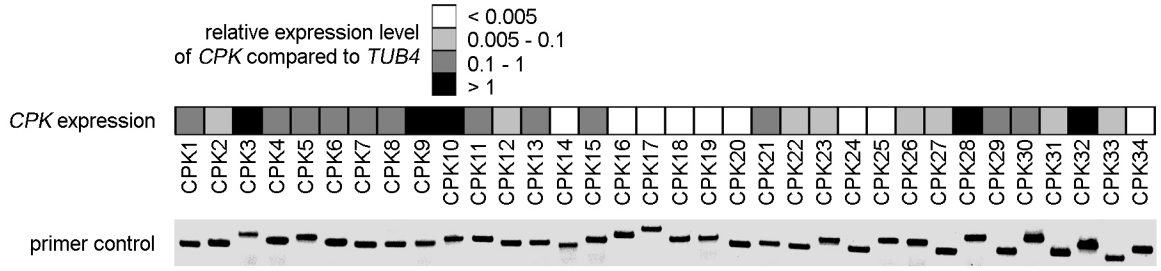

Supplementary Figure 3 | Schematic representation of *CPK* expression in mesophyll protoplasts. The expression level of 34 *CPK* genes was monitored by qRT-PCR. The values were normalized based on the control gene *TUB4* and represented using a color scale for easy visualization (upper panel). The quality of the primers was confirmed using gDNA or cDNA from other plant organs (lower panel). The genes represented with white boxes are barely or not detectable in mesophyll protoplasts. Six of them are predicted to be pollen-specific[1] (*CPK14*, *16*, *17*, *20*, *24* and *34*).

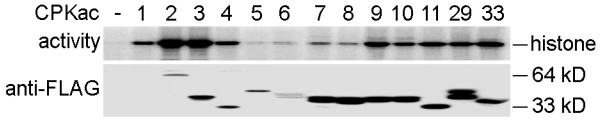

Supplementary Figure 4 | Truncated CPKs are constitutively active. CPKac-FLAG were expressed in protoplasts and immunoprecipitated with anti-FLAG antibody. Kinase activity was measured in vitro, using histone as an artificial substrate, in the presence of EGTA. The expression level of CPKac-FLAG was monitored by immunoblot.

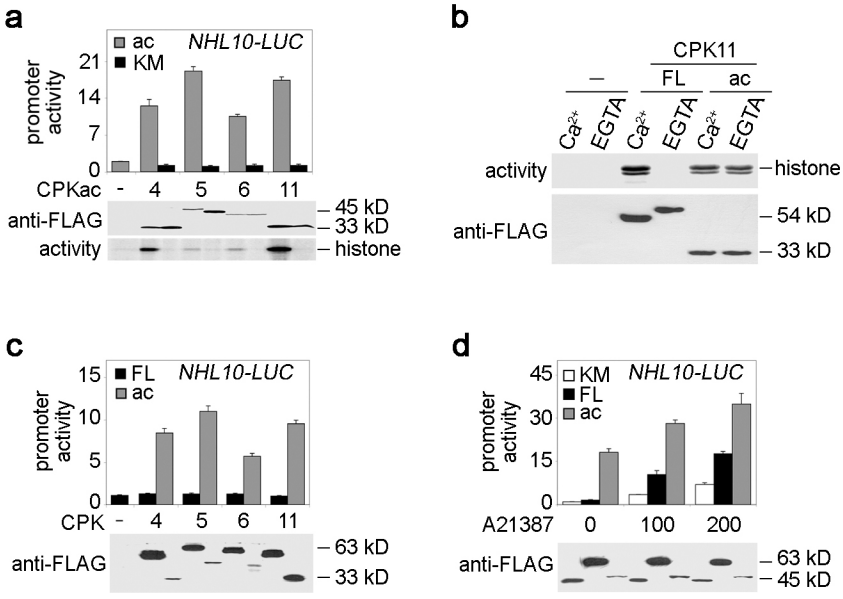

Supplementary Figure 5 | Ca^{2+}-dependent kinase activity of CDPKs is required for flg22 signalling. a, Kinase activity is required for *NHL10-LUC* induction. The constitutively active (ac) and the inactive kinase mutant (KM) of CPKs are compared for *NHL10-LUC* activation, histone phosphorylation activity and protein expression (anti-FLAG). Error bars, s.d. (n=6). **b,** Full-length CPK11 requires Ca^{2+} for activation. The kinase activity and protein expression of full-length (FL) and constitutively active (ac) CPK11 are shown. Ca^{2+} chelater EGTA abolished the phosphorylation activity and Ca^{2+}-dependent mobility shift of CPK11 FL while CPK11ac lacking the EF-hand Ca^{2+}-binding domain and the pseudosubstrate inhibitory region was constitutively active, even in the presence of EGTA, as predicted[2-4]. **c,** Over-expression of full-length CPKs cannot induce *NHL10-LUC*. Promoter activity and CPK protein expression are shown. Error bars, s.d. (n=6). **d,** Full-length CPK5 activity can be enhanced by Ca^{2+} ionophore A23187 in vivo. *NHL10-LUC* induction was measured in protoplasts treated with 1 mM Ca^{2+} without or with 100 or 200 nM ionophore A23187 for 3 h to partially mimic flg22 signalling. Constitutively active CPK5 (ac) is Ca^{2+}-independent but endogenous CDPKs are also activated by A23187. Error bars, s.d. (n=3).

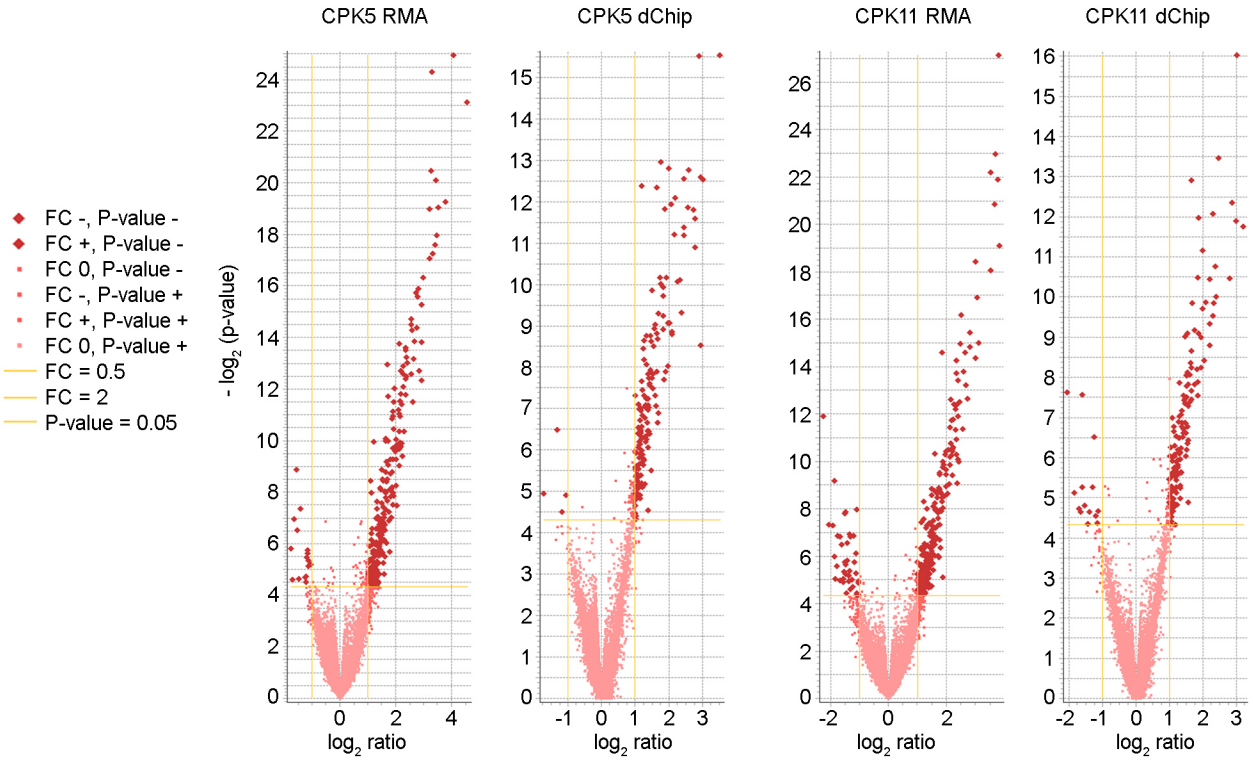

Supplementary Figure 6 | Volcano plots of CPK5ac and CPK11ac target genes. Graphic representation of CPK5ac and CPK11ac target genes using RMA or dChip analysis of microarray data. FC: fold change (Significant activation, FC = 2; significant repression, FC = 0.5), p-value = 0.05.

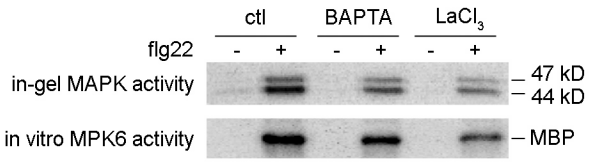

Supplementary Figure 7 | Calcium signalling inhibitors only attenuate MAPK activation by flg22. Protoplasts untransfected (top) or transfected with MPK6-HA (bottom) were treated with 4 mM BAPTA, 2 mM $LaCl_3$ or H_2O control (ctl) for 15 min prior to elicitation with 100 nM flg22 for 15 min. Endogenous MAPK activity was analyzed using an in-gel kinase assay with untransfected protoplasts (top). MPK6-HA was immunoprecipitated from transfected protoplasts with an anti-HA antibody and analyzed for in vitro kinase activity using MBP as a substrate (bottom).

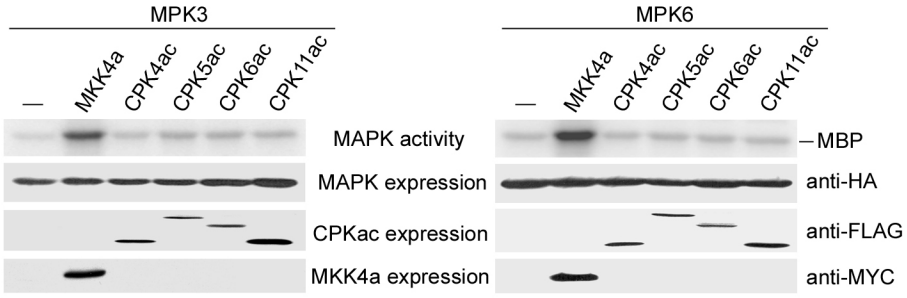

Supplementary Figure 8 | Constitutively active CPKs do not activate MAPKs. Protoplasts co-transfected with MPK3-HA or MPK6-HA and CPKac-FLAG, MKK4a-MYC or control DNA (-) were incubated for 6 h. Immunoprecipitated MAPK-HA was analyzed for in vitro kinase activity using MBP as a substrate. The expression level of MAPK-HA, MKK4a-MYC and CDPKac-FLAG was monitored by immunoblot.

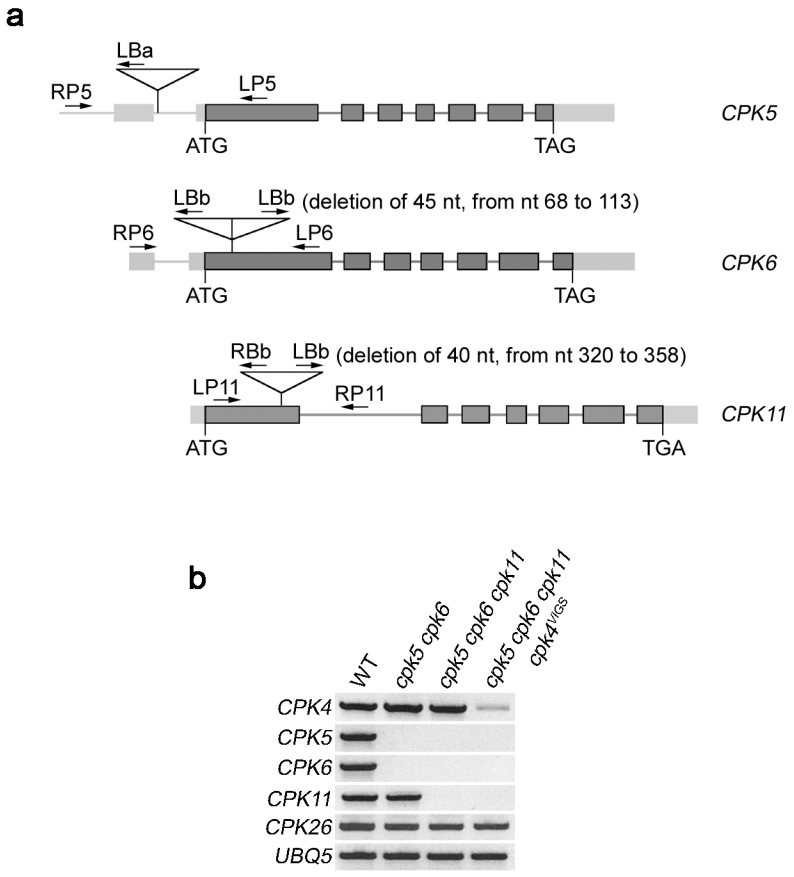

Supplementary Figure 9 | Analysis of *cpk* single mutants. a, T-DNA insertion in the *CPK5* gene (sail_657C06) is in the first intron. As no PCR product could be obtained with LP5 primer, the DNA organization at the RB site could not be determined. In the *cpk6* mutant (salk_025460), 2 copies of T-DNA were inserted in tandem in opposite direction in the first exon, generating a deletion of 45 bp from 68 to 113 bp downstream of the translation start codon (ATG). In the *cpk11* mutant (salk_054495), a single copy of T-DNA was inserted in the first exon, generating a deletion of 40 bp from 320 to 358 bp downstream of the ATG. Lines represent introns while dark and light grey boxes represent exons and UTR regions, respectively. Arrows indicate the primers used for genotyping. Primer sequences are listed in Supplementary Table 14. **b,** *CPK* expression in higher order *cpk* mutants. The *cpk5 cpk6* double and *cpk5 cpk6 cpk11* triple mutants were generated by genetic crosses. The quadruple mutant was generated by introducing a 500-bp *CPK4*-specific construct into the *cpk5 cpk6 cpk11* triple mutant (*cpk5 cpk6 cpk11 cpk4*^{VIGS}) using VIGS[5,6]. A *GFP* gene sequence was used as a control in the other plants (WT, *cpk5 cpk6* and *cpk5 cpk6 cpk11*) to avoid non-specific effect of VIGS. Expression level of *CPK* genes in WT and *cpk* mutants was analyzed by RT-PCR. The T-DNA insertion in *CPK5, 6* and *11* abolished *CPK* expression while *CPK4*-specific VIGS strongly reduced *CPK4* expression. Neither T-DNA insertion or VIGS affected the expression of the closest homolog *CPK26*. The expression of *UBQ5* was used as a control.

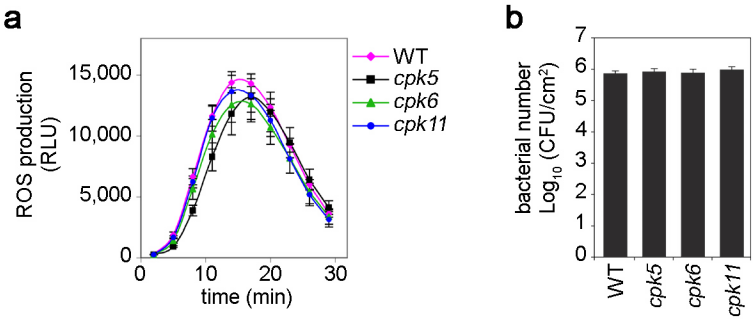

Supplementary Figure 10 | Single *cpk* mutants are not impaired in defense responses. a, Flg22-induced oxidative burst is similar in single *cpk* mutants and WT plants. ROS production was measured in relative light units (RLU) on leaf disks from wild-type (WT), *cpk5*, *cpk6* and *cpk11* mutants after treatment with 100 nM flg22. Error bars, s.d. (n=9). **b,** Single *cpk* mutants display the same sensitivity to the pathogen *Pst* DC3000 as WT plants. Leaves from wild-type (WT), *cpk5*, *cpk6* and *cpk11* mutants were infiltrated with *P. syringae* DC3000 at $5x10^4$ cfu/ml. Bacterial growth was measured 4 days after inoculation (means ± s.d. of three replicates). The experiments were repeated three times with similar results.

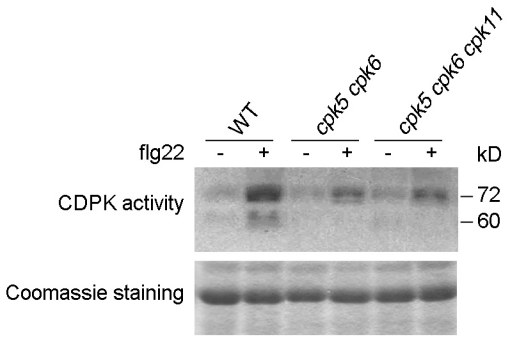

Supplementary Figure 11 | Flg22 activation of 60 kD CDPKs is diminished in *cpk* mutants. CDPK activity was determined by in-gel kinase assay in WT and *cpk* mutant protoplasts treated with 10 nM flg22 for 15 min. The remaining 72 kD CDPK served as a control for specificity. Histone was used as an artificial in vitro substrate for CDPKs. Coomassie staining: protein loading control.

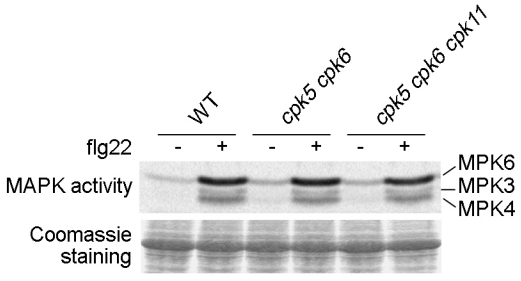

Supplementary Figure 12 | MAPK activation by flg22 is independent of CDPKs. MAPK activity was determined by in-gel kinase assay in seedlings treated with 1 μM flg22 for 15 min. MBP was used as an artificial in vitro substrate for MAPKs. Coomassie staining: protein loading control.

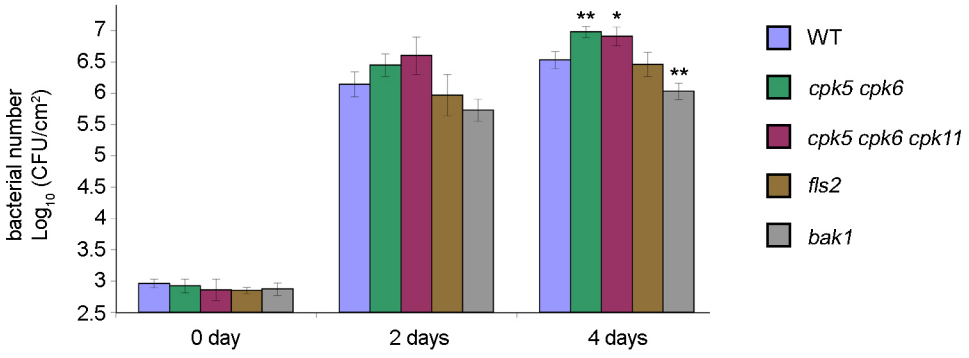

Supplementary Figure 13 | The *cpk* mutants are more susceptible to the bacterial pathogen *Pst* DC3000. Leaves from WT (Col-0), *cpk*, *fls2* and *bak1* mutants were infiltrated with *Pst* DC3000 at $5x10^4$ cfu/ml and bacterial growth was measured at indicated times. Error bars, s.d. (n=3). The differences are significant with $p < 0.03$ (**) or $p < 0.05$ (*) when compared with data from WT at the same time point based on the results of an unpaired Student's t-test.

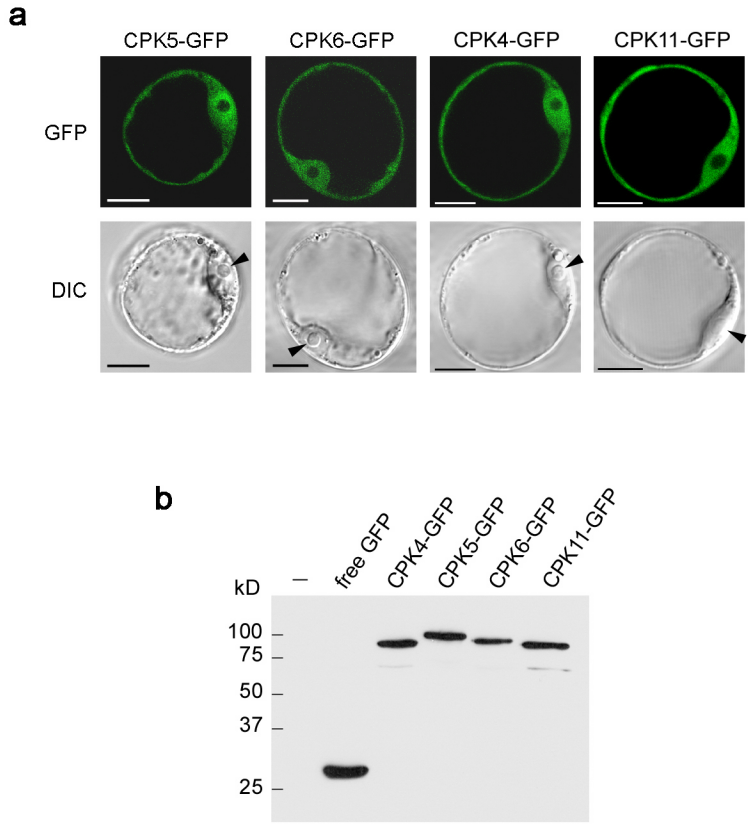

Supplementary Figure 14 | The four CPK-GFP are localized in both cytoplasm and nucleus. a, Subcellular localization of CPK-GFP fusion proteins. Specific constructs were expressed in protoplasts from Arabidopsis suspension cells for clear organelle visualization. GFP: GFP fluorescence, DIC: Differential interference contrast microscopy. The arrows indicate the nucleolus inside the nucleus. Scale bars are 15 μm. **b,** CDPK-GFP are not processed in transfected protoplasts. Proteins from protoplasts transfected with free GFP or CPK-GFP were analyzed by immunoblot with an anti-GFP antibody. Free GFP was not detected in protoplasts expressing CPK-GFP, confirming that the CPK-GFP localization observed using confocal microscopy corresponds to the fusion proteins.

SUPPLEMENTARY TABLES

Supplementary Table 1 | Expression level of *CPK* genes relative to *TUB4* in mesophyll cell protoplasts. The expression level of *CPK* genes was monitored by qRT-PCR and was assigned the value « 0 » when no PCR product was obtained from mesophyll cell protoplasts. The quality of the primers was checked on genomic DNA or cDNA from other organs (Supplementary Fig. 3).

Gene	AGI Number	Expression level
CPK1	At5g04870	0.33742 ± 0.12665
CPK2	At3g10660	0.01268 ± 0.00540
CPK3	At4g23650	3.56092 ± 1.83776
CPK4	At4g09570	0.61783 ± 0.16329
CPK5	At4g35310	0.71715 ± 0.24428
CPK6	At2g17290	0.36733 ± 0.06499
CPK7	At5g12480	0.62047 ± 0.24023
CPK8	At5g19450	0.19490 ± 0.02657
CPK9	At3g20410	2.15086 ± 1.20276
CPK10	At1g18890	1.13954 ± 0.36701
CPK11	At1g35670	0.42881 ± 0.15127
CPK12	At5g23580	0.07002 ± 0.01054
CPK13	At3g51850	0.29619 ± 0.09337
CPK14	At2g41860	0.00010 ± 0.00004
CPK15	At4g21940	0.54500 ± 0.24620
CPK16	At2g17890	0.00027 ± 0.00009
CPK17	At5g12180	0.00004 ± 0.00002
CPK18	At4g36070	0.00183 ± 0.00077
CPK19	At1g61950	0
CPK20	At2g38910	0.00021 ± 0.00020
CPK21	At4g04720	0.13906 ± 0.01492
CPK22	At4g04710	0.00567 ± 0.00163
CPK23	At4g04740	0.03803 ± 0.01307
CPK24	At2g31500	0.00359 ± 0.00059
CPK25	At2g35890	0.00009 ± 0.00004
CPK26	At4g38230	0.06429 ± 0.01271
CPK27	At4g04700	0.02331 ± 0.00449
CPK28	At5g66210	2.41219 ± 0.87689
CPK29	At1g76040	0.29004 ± 0.16224
CPK30	At1g74740	0.37729 ± 0.15709
CPK31	At4g04695	0.05700 ± 0.01844
CPK32	At3g57530	1.54108 ± 0.62045
CPK33	At1g50700	0.05899 ± 0.01538
CPK34	At5g19360	0.00192 ± 0.00035

Supplementary Table 2 | CPK5 and CPK11 target gene list. The Supplementary Table 2 is available as a Microsoft Excel file. Shared target genes between CDPK and flg22 are marked in green.

Supplementary Table 3 | Shared CPK5 and CPK11 target genes overlapping with early flg22 responsive genes. The Supplementary Table 3 is available as a Microsoft Excel file.

Supplementary Table 4 | Specific CPK5 target genes overlapping with early flg22 responsive genes. The Supplementary Table 4 is available as a Microsoft Excel file.

Supplementary Table 5 | Specific CPK11 target genes overlapping with early flg22 responsive genes. The Supplementary Table 5 is available as a Microsoft Excel file.

Supplementary Table 6 | CPK5 and CPK11 target genes overlapping with early flg22 responsive genes in Arabidopsis protoplasts, leaves and seedlings. The data in Supplementary Table 6 is visualized in Fig. 2a and available as a Microsoft Excel file.

Supplementary Table 7 | CPK5 and CPK11 target genes overlapping with early MAMP responsive genes in Arabidopsis leaves and seedlings. The data in Supplementary Table 7 is visualized in Fig. 2b and available as a Microsoft Excel file.

Supplementary Table 8 | CPK5 and CPK11 target genes overlapping with microbe responsive genes in Arabidopsis leaves. The data in Supplementary Table 8 is visualized in Fig. 2c and available as a Microsoft Excel file.

Supplementary Table 9 | Sequences of oligonucleotide primers for CPKac cloning. The cloning sites (BamHI, BglII, StuI) are italicized. F: forward; R: reverse.

Gene	AGI Number	Primer
CPK1	At5g04870	F: GA*AGATCT*ATGGGTAATACTTGTGTTGG
		R: AAA*AGGCCT*CACACCGTCGACTTGAAC
CPK2	At3g10660	F: CGC*GGATCC*ATGGGTAATGCTTGCGTT
		R: AAA*AGGCCT*CACACCGTCAATCTGTAC
CPK3	At4g23650	F: CGC*GGATCC*ATGGGCCACAGACACAGC
		R: AAA*AGGCCT*CTCCCCATCTTCTCTAAT
CPK4	At4g09570	F: CGC*GGATCC*ATGGAGAAACCAAACCCT
		R: AAA*AGGCCT*AGCATGTTCATCAACAATC
CPK5	At4g35310	F: CGC*GGATCC*ATGGGCAATTCTTGCC
		R: AAA*AGGCCT*AACACCATTCTCACAGATC
CPK6	At2g17290	F: TCCCCCG*GGATCC*ATGGGCAATTCATGTCGT
		R: CCGCTCGAG*AGGCCT*AACTCCATTCTCACAGAT
CPK7	At5g12480	F: CGC*GGATCC*ATGGGGAATTGTTGTGG
		R: AAA*AGGCCT*CTTCTTTGCATTCAGTATCC
CPK8	At5g19450	F: CGC*GGATCC*ATGGGAAATTGTTGTGCG
		R: AAA*AGGCCT*CTTCTTCGCATTTTGTATCC
CPK9	At3g20410	F: CGC*GGATCC*ATGGGAAATTGTTTTGCC
		R: AAA*AGGCCT*TTCTCCACCTTCTCTAAGCC
CPK10	At1g18890	F: CGC*GGATCC*ATGGGTAACTGTAACGCC
		R: AAA*AGGCCT*TTTCTTTGCATTCTGTATC
CPK11	At1g35670	F: CGC*GGATCC*ATGGAGACGAAGCCAAAC
		R: AAA*AGGCCT*TGCTTGTTCATCGACAAT
CPK12	At5g23580	F: CGC*GGATCC*ATGGCGAACAAACCAAGA
		R: AAA*AGGCCT*AACCTTATCATCCACAAT
CPK13	At3g51850	F: CGC*GGATCC*ATGGGAAACTGTTGCAGA
		R: AAA*AGGCCT*TTTCTTTGCGTTCTGAAT
CPK15	At4g21940	F: CGC*GGATCC*ATGGGTTGCTTTAGCAGC
		R: AAA*AGGCCT*TTCTCCTCCTCTGATCCA
CPK21	At4g04720	F: CGC*GGATCC*ATGGGTTGCTTCAGCAGT
		R: AAA*AGGCCT*TTCTCCCCCTTTGATCCA
CPK22	At4g04710	F: CGC*GGATCC*ATGGGTAATTGCTGCGGA
		R: AAA*AGGCCT*TTCGCTTTTCATCCATGG
CPK23	At4g04740	F: CGC*GGATCC*ATGGGTTGTTTCAGCAGT
		R: AAA*AGGCCT*TTCTCCCCCTTTGATCCA
CPK26	At4g38230	F: CGC*GGATCC*ATGAAGCACAGCGGTGG
		R: AAA*AGGCCT*AACTCCATTTTCACAGATCC

CPK27	At4g04700	F: CGC*GGATCC*ATGGGTTGCTTCAGCAGT
		R: AAA*AGGCCT*TTCTCCTTCTTTCATCCAAG
CPK28	At5g66210	F: CGC*GGATCC*ATGGGTGTCTGTTTCTCCG
		R: AAA*AGGCCT*ATTCCCGCCTTCTCTAACC
CPK29	At1g76040	F: CGC*GGATCC*ATGCTTCAAAACCAACAT
		R: AAA*AGGCCT*TTTGGTGTCTGTCATCCA
CPK30	At1g74740	F: CGC*GGATCC*ATGGGTAATTGTATCGCC
		R: AAA*AGGCCT*TTTCTTTGCATTCTGTATC
CPK31	At4g04695	F: CGC*GGATCC*ATGGGTTGCTACAGCAGT
		R: AAA*AGGCCT*TTCTCCGTCTTTCATCCAAGGA
CPK32	At3g57530	F: CGC*GGATCC*ATGGGTAATTGTTGCGG
		R: AAA*AGGCCT*TGTCTTTGCATTCTGTAACC
CPK33	At1g50700	F: CGC*GGATCC*ATGGGGAATTGCTTAGC
		R: AAA*AGGCCT*TTCTCCACCTTCTCTTAGC

Supplementary Table 10 | Sequences of oligonucleotide primers for site-directed mutagenesis of CPKac to generate the kinase mutant (KM). F: forward; R: reverse.

Gene	Mutation	Primer
CPK4	K54M	F: CTAATTACGCTTGCATGTCAATCCCAAAACG
		R: CGTTTTGGGATTGACATGCAAGCGTAATTAG
CPK5	K126M	F: TTGACTACGCTTGTATGTCAATATCCAAGAG
		R: CTCTTGGATATTGACATACAAGCGTAGTCAA
CPK6	K114M	F: TTGACTATGCTTGTATGTCTATATCCAAGAG
		R: CTCTTGGATATAGACATACAAGCATAGTCAA
CPK11	K55M	F: CTAATTACGCCTGCATGTCGATCCCGAAGCG
		R: CGCTTCGGGATCGACATGCAGGCGTAATTAG

Supplementary Table 11 | Sequences of oligonucleotide primers for FL CPK cloning. The cloning sites (BamHI, StuI) are italicized. F: forward; R: reverse.

Gene	AGI Number	Primer
CPK4	At4g09570	F: CGC*GGATCC*ATGGAGAAACCAAACCCT
		R: GA*AGGCCT*CTTTGGTGAATCATCAGA
CPK5	At4g35310	F: CGC*GGATCC*ATGGGCAATTCTTGCC
		R: GA*AGGCCT*CGCGTCTCTCATGCTAAT
CPK6	At2g17290	F: TCCCCCG*GGATCC*ATGGGCAATTCATGTCGT
		R: GA*AGGCCT*CACATCTCTCATGCTGAT
CPK11	At1g35670	F: CGC*GGATCC*ATGGAGACGAAGCCAAAC
		R: GA*AGGCCT*GTCATCAGATTTTTCACCAT

Supplementary Table 12 | Sequences of oligonucleotide primers for qRT-PCR.

F: forward; R: reverse.

Gene	AGI Number	Primer
CPK1	At5g04870	F: AGACAATGACGGGCGAATAG
		R: TGATGCTTCCTTTCTGCATC
CPK2	At3g10660	F: CAAGACAAGGATGGACGAATAG
		R: CCATTATGCTCCCTTTCTGC
CPK3	At4g23650	F: TGACAACAGCGGCTACATAAC
		R: ACGATCGGTGTCTACTTCAGC
CPK4	At4g09570	F: CTTGATAATGACGGGAAGATTG
		R: AGTTCTGCTCCTCCCAACAC
CPK5	At4g35310	F: TATGGATGCGGCTGATGTAG
		R: GCTCTTCCCGCTCTAGTTTG
CPK6	At2g17290	F: AGACAACGATGGACGGATTG
		R: CTCCCTACACCAGCATTTCC
CPK7	At5g12480	F: CGACAAGGATGGACGAATAAG
		R: TCCAATCTGTCCCAGCTTTC
CPK8	At5g19450	F: GATGGAAGCTGCTGATGTTG
		R: GCACAGAGACAGCCACAAAC
CPK9	At3g20410	F: CGACTCCGATAACGATGGTAG
		R: CGAGGTTGTTGTTGTTGTGG
CPK10	At1g18890	F: GGGAAGCTTTAGCGGATGAG
		R: TACGTCCGTCCTTGTCAGTG
CPK11	At1g35670	F: GCATTACGGGTAATTGCTGAG
		R: GTTCCGCTGTTGTCTGTGTC
CPK12	At5g23580	F: GTGCGGCTGATGTTGATG
		R: TGTTCAAGTGGATTGTTGCAG
CPK13	At3g51850	F: TGAAGCGGTGGATACTAAAGG
		R: TTGCAGGTGGAGAGACACTG
CPK14	At2g41860	F: GATGTCGATACCAATAAGGATGG
		R: TTTCATCATCGTTGCAAATTC
CPK15	At4g21940	F: GTCGATACAGATAACGATGGAAG
		R: TTGTTGTGGCAGTGTGATACC
CPK16	At2g17890	F: AACACGATTCCGAGAAGTGG
		R: CCAGTATGCATTCGAAGTTCC
CPK17	At5g12180	F: TGCATTACGGGTGATAGCAG
		R: TCTGACAACCTTGTACCTTGC
CPK18	At4g36070	F: TCCAAGCGAATGATAGCAAC
		R: CAATTGGTTCACGTGCAAAG
CPK19	At1g61950	F: TTGATGCTGATAATGATGGAAG
		R: TTGATTGGTGTGATTGTGAGC
CPK20	At2g38910	F: GTCGATAAAGACAACGATGGAAG
		R: CAGTGTCTTGCATCATATCCAC
CPK21	At4g04720	F: CTGTGTTATCCCGCATGAAG
		R: TCCGCGATAACCTTTAGAGC
CPK22	At4g04710	F: AAGCGGGCACATAACGAAG
		R: TTCATCTCCCATACCATGCTC

CPK23	At4g04740	F: TGAAGCGTCTGATGTGGATG
		R: TTGTGTACGTGCTCATCGTG
CPK24	At2g31500	F: CAACAAGGATGGACGGATAAG
		R: AATCCGTCCCTGATTTCATC
CPK25	At2g35890	F: TGCAAATACCAACGGATGTG
		R: AACGATCATTTGCTTCCTCTTC
CPK26	At4g38230	F: CGACCAAGACAATGATGGAAG
		R: TTCCTGATGCTCATGTTTATGC
CPK27	At4g04700	F: GTGAAAGAACCTGAGGGACAG
		R: CCTCGCTGTAGTCGATTTCC
CPK28	At5g66210	F: GAGGAACTTCGAATGCACAC
		R: GCTTGGTGCTCTCTGTGAAC
CPK29	At1g76040	F: ATGGAAGCTGCTGATGTGG
		R: ATGACGATGCATTGTTGCAG
CPK30	At1g74740	F: GGAAGTGGCGGATGTTAATG
		R: CTGATTCGATGTATCCACTTCC
CPK31	At4g04695	F: ACAATGACGGGCACATAACC
		R: GCTAACTTCATCTCCCACACC
CPK32	At3g57530	F: GATGCTGGAGACATCGATAGAG
		R: AGAACGCAAACGCTTTCTTG
CPK33	At1g50700	F: CGCTGATAATGACGGTAGAATC
		R: TTCCCACTTCTCATCATAGCAC
CPK34	At5g19360	F: AGCTAGAGCAAGCCCTTCG
		R: AGTTTATCCGCCCATCATTG
TUB4	At5g44340	F: AGGGAAACGAAGACAGCAAG
		R: GCTCGCTAATCCTACCTTTGG
EIF4a	At3g13920	F: TCATAGATCTGGTCCTTGAAACC
		R: GGCAGTCTCTTCGTGCTGAC
PHI1	At1g35140	F: TTGGTTTAGACGGGATGGTG
		R: ACTCCAGTACAAGCCGATCC
FRK1	At2g19190	F: CGGTCAGATTTCAACAGTTGTC
		R: AATAGCAGGTTGGCCTGTAATC
NHL10	At2g35980	F: TTCCTGTCCGTAACCCAAAC
		R: CCCTCGTAGTAGGCATGAGC
PER62	At5g39580	F: GCGATCTCGTCACTCTTGTTG
		R: CGTGATAAACCCACATGCAG
PER4	At1g14540	F: CGTTTAGGGCTATCGCAGAC
		R: ACGTGAGGCATTGAGCTTG
CYP82C2	At4g31970	F: AATCTACCTGCCTGGCACTG
		R: GAGAAATGGCCCATGTAAGG
CYP81F2	At5g57220	F: AAATGGAGAGAGCAACACAATG
		R: ATCGCCCATTCCAATGTTAC
WAK2	At1g79680	F: CGTGTGAGTACACAAATCATCG
		R: TGGTTTAACCTCCTTTGTCTTC
FOX	At1g26380	F: GGCTGCACTTCAACCCTTAC
		R: TTACTCTCTGTGGCGTTTGG

Supplementary Table 13 | Sequences of oligonucleotide primers for semi-quantitative RT-PCR. F: forward; R: reverse.

Gene	AGI Number	Primer
NHL10	At2g35980	F: ACCTAGCCCTCACTGTTCCTGT
		R: TAAACCTAACCCTAAGCCTGAA
UBQ5	At3g62250	F: GTGGTGCTAAGAAGAGGAAGA
		R: TCAAGCTTCAACTCCTTCTTT
CPK4	At4g09570	F: TCCATACGAAACACCAAGA
		R: GTTCCTCATAGTTCTGCTCC
CPK5	At4g35310	F: GACGAAGGCGATAACAATAA
		R: CCGCTCTAGTTTGTTGAGAT
CPK6	At2g17290	F: AAATCCACCACCACTACTGT
		R: ACTGAAATGCAGAGACAAGAT
CPK11	At1g35670	F: GAGACGAAGCCAAACCCTA
		R: GCTGTAAACTCCGAGAAATC
CPK12	At5g23580	F: CAGATGGGTTCTTCCTTACA
		R: CTCATAGTTCTCCGACCAAT
CPK26	At4g38230	F: CTCTACTCGTTGGGACACA
		R: CCGTAGTCAATCCTTCCA

Supplementary Table 14 | Sequences of oligonucleotide primers for genotyping *cpk* mutants. LP: left primer; RP: right primer; LB: left border primer; RB: right border primer.

Gene	AGI Number	Primer
CPK5	At4g35310	LP5: TCGTTCCAAATTGACCTTGAC
		RP5: GAGGAAACAGCGGAGAGAGAC
CPK6	At2g17290	LP6: CTCGCAACTAACGCTTACCTG
		RP6: TTTTGGGATCTATAATGATCGATG
CPK11	At1g35670	LP11: AAATGATGGTGTTTTTATTTATGTAAAG
		RP11: AAACCAATTAGGCGATGAACC
T-DNA sail		LBa: TTCATAACCAATCTCGATACAC
T-DNA salk		LBb: GCGTGGACCGCTTGCTGCAACT
		RBb: GTTTCTGACGTATGTGCTTAGC

SUPPLEMENTARY METHODS

DNA constructs. All primers used for cloning and mutagenesis are listed in Supplementary Tables 9-11 and PCR products were checked by sequencing. Effector constructs of full-length (FL) or constitutively active CDPKs (CPKac) were generated by inserting the cDNA (including the first ATG) in a plant expression vector containing a FLAG epitope tag or GFP at the C-terminus, between a 35S-derived promoter and NOS terminator[4,7-10]. The sequence between the promoter and the first ATG of each CDPK contains 8 nucleotides, including the BamHI restriction site for cloning and no additional ATG, which supports the translation to start at the first ATG of CDPKs. Sequencing validated that no additional amino acids were added to the N-terminus of CDPKs by the vector. The cDNA was amplified from Arabidopsis plants Col-0. The constructs for inactive kinase mutant (KM) forms of CDPK were generated using site-directed mutagenesis to replace the conserved lysine residue of the ATP-binding domain with a methionine. The effector constructs FLS2-HA, MKK4a-MYC, MPK3-HA and MPK6-HA have been previously described[7]. For VIGS, the *CPK4* construct was generated using a gene specific 500-bp fragment of the coding region that was cloned with the primers 5'-GGAATTCAACACCAAGATTAAGAGA-3' and 5'-GGGGTACCACAGATACTGCCCTGGCT-3'.

In-gel protein kinase assays. For in-gel kinase assay of endogenous MAPKs, 10-day-old seedlings were ground in liquid nitrogen and homogenized in 150 µl extraction buffer (50 mM HEPES-KOH pH 7.5, 5 mM EDTA, 5 mM EGTA, 2 mM DTT, 25 mM β-glycerophosphate, 2 mM Na_3VO_4, 10 mM NaF, 1 mM PMSF, 5

μg/ml antipain, 5 μg/ml leupeptin). The protein extract was recovered after centrifugation at 17600 g for 15 min at 4°C. Equal amounts of proteins were loaded on 10% SDS-polyacrylamide gel embedded with 0.25 mg/ml myelin basic protein (MBP, Invitrogen). The gel was washed 3 times with washing buffer (25 mM Tris-HCl pH=7.5, 0.5 mM DTT, 5 mM NaF, 0.1 mM Na_3VO_4, 0.5 mg/ml BSA, 0.1% Triton X-100), then incubated for 16 h with 3 changes in renaturation buffer (25 mM Tris-HCl pH 7.5, 0.5 mM DTT, 5 mM NaF, 0.1 mM Na_3VO_4) at 4°C. After a 30 min preincubation at room temperature in the reaction buffer (25 mM Tris-HCl pH 7.5, 1 mM DTT, 0.1 mM Na_3VO_4, 12 mM $MgCl_2$, 1 mM EGTA), the kinase reaction was performed for 1 h in the reaction buffer supplemented with 25 μM cold ATP and 50 μCi [□-^{32}P] or [□-^{33}P] ATP. The reaction was stopped by extensive washes in 5% TCA and 1% sodium pyrophosphate for 6 h. The protein kinase activity was detected on dried gel by the Typhoon imaging system (GE Healthcare).

For in-gel kinase assay of endogenous CDPKs, protoplasts were directly resuspended in SDS sample buffer. Proteins were loaded on 10% SDS-polyacrylamide gel embedded with 0.25 mg/ml histone III-S (Sigma). The gel was treated for washing, renaturating and reaction steps as described above, with the following modifications□ the reaction buffer contains 25 mM Tris-HCl pH 7.5, 1 mM DTT, 0.1 mM Na_3VO_4, 12 mM $MgCl_2$, 1 mM $CaCl_2$ and no cold ATP was added during the kinase reaction.

In vitro protein kinase assays. For in vitro kinase assay, protoplasts were lysed in 200 μl immunoprecipitation (IP) buffer (50 mM Tris-HCl pH 7.5, 150 mM NaCl, 5 mM EDTA, 1 mM DTT, 2 mM NaF, 2 mM Na_3VO_4, 1X cocktail inhibitor [Roche], 1% Triton X-100). To immunoprecipitate CPK-FLAG, protein extracts were incubated with anti-FLAG antibody at 4°C for 2 h, and additional 1 h after adding 15

µl protein G sepharose beads (GE Healthcare). The immunoprecipitated kinases were washed twice with IP buffer and once with kinase buffer (20 mM Tris-HCl pH=7.5, 15 mM $MgCl_2$, 1 mM $CaCl_2$ or 5 mM EGTA, 1 mM DTT). Kinase reaction was performed for 30 min in 15 µl kinase buffer containing 1 µg histone (Sigma), 50 µM cold ATP and 2 µCi [□-^{32}P] or [□-^{33}P] ATP. The reaction was stopped by adding SDS-PAGE loading buffer. After separation on 10% SDS-PAGE, radiolabelled histone was detected on dried gel by the Typhoon imaging system (GE Healthcare). For MAPK activity, immunoprecipitation was carried out with anti-HA antibody, and the kinase reaction was performed with 5 mM EGTA and 1 µg MBP.

Bacterial growth assays. The bacterial growth assays were performed as previously described in leaf[8] and seedlings[11] with some modifications. For leaf assay, an overnight culture of *Pseudomonas syringae pv tomato* DC3000 was washed and resuspended to 5x10^4 cfu/ml in H_2O. Arabidopsis leaves of 4-week-old plants were infiltrated with bacteria using a needleless syringe. Two and four days after inoculation, leaf disks were ground in 100 µl H_2O and serial dilutions were plated on KB medium. Bacterial cfu were counted 2 days after incubation at 28°C. For seedling assay, seedlings were grown in 6-well plates containing 1 ml of liquid medium (0.5 x MS, 0.5% sucrose) for 5 days under continuous light at 22°C. Seedlings were treated with 100 nM flg22 for 1 day prior to inoculation with *Pst* DC3000 at a final concentration of 1x10^7 cfu/ml. After 3 days of co-cultivation, seedlings were surface sterilized with 70% ethanol and rinsed with H_2O before grinding tissues for bacterial counting as above. The experiments were repeated three times with similar results.

Microarray quality assessment. For microarrays processed at The Partners HealthCare Center for Personalized Genetic Medicine Microarray Facility, the array data quality was initially assessed in R using the BioConductor package arrayQualityMetrics[12]. In addition, the BioConductor package Harshlight[13] was used to provide assessment of possible large scale artefacts, and R code for SmudgeMiner[14] was used for assessment of possible spatial bias. Affymetrix ATH1 GeneChip data were generated from duplicate or triplicate biological samples.

Comparison of various data processing methods. To define CPK5ac and CPK11ac target genes with high stringency and statistical significance, we processed and compared the ATH1 GeneChip data using various microarray analysis and statistic algorithms[15-17]. Affymetrix probe level data for control, CPK5ac and CPK11ac in the form of .CEL files were loaded into FlexArray[18] and examined and preprocessed with various algorithms, including RMA[19,20], dChip[21] (both with adjustment of PM values, PMMM, and without adjustment to PM values, PM-only), and MAS 5.0[15,17,22]. Each of the resulting analysis was then further processed on a gene level with regard to probability of change with respect to variability across duplicate arrays. This was done using the t-test as well as an adaptation of the t-test, SAM (Significance Analysis of Microarrays)[23], and a Bayesian version of the t-test, cyber-T[24]. Cyber-T is a version of the t-test that uses a Bayesian estimate of the treatment variance (window size of 101 and confidence ratio of 10 was used). In SAM, the statistic test computed for each gene is slightly different from the t-test in that it includes a factor in the denominator selected to minimize the coefficient of variation across arrays, and is also intended to guard against unrealistically small estimates of variability occasionally observed due to low sample size. Also, SAM does not use the

hypothetical t-distribution to assess significance of observed effects, but permutations of the data set generate an empirical null distribution. Significance is evaluated using this alternative null as a reference (100 permutations and a random number seed of 0 was used).

Affymetrix probe level data for control, CPK5ac and CPK11ac were also analyzed using Gene Chip Operating Software (GCOS)[25]. Each Affymetrix array hybridization resulting from CPK5ac or CPK11ac RNA samples was compared to two separate Affymetrix arrays with control RNA from different biological experiments. A target signal of 1500 was used with default GCOS parameters[25]. Regulated genes were then determined by removing genes consistent with the following criteria: a change call of 'no change'; a signal $\log_2$ ratio between -0.99 and 0.99 (less than two-fold change in expression); a detection call of absent in both control and treatment arrays. Because three separate algorithms are used in GCOS to determine detection, change, and signal value[25], there can be occasional discrepancies between the results of these algorithms. Genes showing these discrepancies were eliminated under the two additional criteria: a change call of 'increase' or 'marginal increase' combined with either a signal $\log_2$ ratio less than 0, an absent call in the CPK5ac or CPK11ac array, or a signal value in the control RNA array that was greater than the signal value in the CPK5ac or CPK11ac array; a change call of 'decrease' or 'marginal decrease' combined with either a signal $\log_2$ ratio greater than 0; an absent call in the control RNA array, or a signal value in the control that was less than the signal value in the CPK5ac or CPK11ac array.

After comparing the results from the extensive analyses of control, CPK5ac and CPK11ac arrays, it was found that RMA[19,20] with cyber-T[24] and a p-value cutoff of 0.05 was most in agreement with our qRT-PCR data for the validation of eight

marker genes (n=6) in triplicate biological samples (Fig. 3). The combination of RMA[19,20] followed by cyber-T[24] (a p-value cutoff of 0.05) was chosen to analyze arrays for 30 min and 60 min flg22 treatment in protoplasts and seedlings (Fig. 2a) as well as arrays for MAMP signals (Fig. 2b) and microbial infection (Fig. 2c) downloaded from the public domain.

Identification of CPK5ac-specific, CPK11ac-specific, and common CPK5ac and CPK11ac target genes. Arrays for CPK5ac and CPK11ac along with respective control arrays were analyzed in FlexArray[18] using RMA[19,20] followed by cyber-T[24] as well as dChip[21] followed by cyber-T[24]. Candidate target genes were chosen from each of the two analysis based on a p-value of 0.05 or less (Supplementary Fig. 6). Significant target genes separately showed a p-value of 0.05 and $\log_2$ ratio >1 or <-1 in both RMA and dChip processing (Supplementary Table 2). The p-values of majority (93%) of these target genes were below 0.03. The p-value of 0.05 was accepted to cover the validated marker gene *CYP82C2* (Fig. 3, 4a), which had relatively low expression level, thus high variance. They were categorized as CPK5ac-specific (72 genes), CPK11ac-specific (59 genes), or common CPK5ac and CPK11ac (113 genes) target genes (Supplementary Table 2). The functional description of the listed genes is based on TAIR 8.0. Functional descriptions were downloaded from the TAIR website (ftp://ftp.arabidopsis.org/Genes/TAIR8_genome_release/TAIR8_functional_descriptions), Mapman[26] and the Sheen lab annotation[6] (http://genetics.mgh.harvard.edu/sheenweb/search_affy.html).

Identification of CPK5ac and CPK11ac target genes as early flg22 responsive genes. Duplicate or triplicate microarray data from three separate conditions of flg22 treatments in protoplasts (30 min and 60 min) (see online METHODS), seedlings (30 min and 60 min) (see online METHODS) and 5-week-old adult leaves (60 min) from Columbia ecotype (http://arabidopsis.org/info/expression/ATGenExpress.jsp, and see below) were collected. Resulting array data was assessed for quality as described above. Affymetrix .CEL files for protoplasts, seedlings and leaves were then imported into FlexArray[18] and processed with RMA[19,20] followed by cyber-T[24]. Flg22 responsive genes were selected by the criteria of p-value of 0.05 or less after processing with RMA[19,20] followed by cyber-T[24].

After processing, all data were imported into Excel. VBA scripts were then used to extract CDPK target genes from the protoplast, leaf, and seedling data for early flg22 responsive genes. The resulting list of candidate flg22-CDPK early target genes (Supplementary Table 2) was then selected manually by eliminating genes that met the following criteria: genes not regulated in any of the flg22 conditions; genes with a CDPK signal $\log_2$ ratio of between -1 and 1; genes that were reverse regulated between CDPK and flg22. Three gene lists resulted; common CPK5ac and CPK11ac target genes that were also early flg22 responsive genes (81 genes) (Fig. 2a, Supplementary Table 3); CPK5ac-specific genes that were also early flg22 responsive genes (59 genes) (Fig. 2a, Supplementary Table 4), CPK11ac-specific genes that were also early flg22 responsive genes (31 genes) (Fig. 2a, Supplementary Table 5). The resulting gene lists were presented using Hierarchical Clustering analysis in Cluster 3.0[27] and Java TreeView 1.1.3[28] (Fig. 2a, Supplementary Table 6) as described below.

Comparison of flg22-CDPK early target genes with early MAMP responsive genes. Duplicate or triplicate microarray data from various MAMP treatments (elf26[29], chitin[30], harpin[31], NPP1[32,33] and LPS[34]) for 30 min, 60 min or 4 h in seedlings or leaves were downloaded from various public domain sources while data for PGN[35] treatment was kindly provided by A. Gust and T. Nürnberger (see below). ABA early (60 min) genes in seedlings were used as a microarray control. Affymetrix .CEL files were imported into FlexArray[18] and processed with RMA[19,20] followed by cyber-T[24]. Early MAMP responsive genes were selected by the criteria of p-value of 0.01 or less. After processing, all data were imported into Excel. VBA scripts were then used to extract genes from the RMA-cyber-T processed MAMP data using the list of 171 flg22-CDPK early target genes (Supplementary Tables 2-5). The resulting gene lists were presented using Hierarchical Clustering analysis in Cluster 3.0[27] and Java TreeView 1.1.3[28] (Fig. 2b, Supplementary Table 7) as described below.

Comparison of flg22-CDPK early target genes with genes regulated by microbial infection. Microarray data from microbial exposure to *Pseudomonas syringae pv. phaseolicola*, *P. infestans*, and *B. cinerea*[36] were downloaded from various public domain sources (see below). Affymetrix .CEL files were imported into FlexArray[18] and processed with RMA[19,20] followed by cyber-T[24]. Regulated genes were selected by the criteria of p-value of 0.01 or less. After processing, data were imported into Excel. VBA scripts were then used to extract genes from the RMA-cyber-T processed microbial infection data using the list of 171 flg22-CDPK early target genes (Supplementary Tables 3-5). The resulting genes lists were presented using Hierarchical Clustering analysis in Cluster 3.0[27] and Java TreeView 1.1.3[28] (Fig. 2c, Supplementary Table 8) as described below.

Clustering of data

Gene lists with signal log ratio values, $\log_2$ (fold-change), were imported into Cluster 3.0[27] for Hierarchical Clustering analysis using binary, agglomerative, hierarchical centroid linkage clustering with a Pearson correlation similarity metric for genes. More specifically, Correlation (uncentered), a modified Pearson correlation in which the mean is assumed to be 0, was the similarity metric chosen. The resulting clustering was viewed with Java TreeView 1.1.3[28] (Fig. 2).

ATH1 GeneChip data from public domains

All the original data for 18 ATH1 GeneChips generated for this project were submitted to Gene Expression Omnibus (GEO) microarray database at National Centre for Biotechnology Information (NCBI) for public access.

Flg22

Leaf data for flg22 (1 μM, 60 min) were obtained from the AtGenExpress project: B20-ATGEN, B34-ATGEN, and B6-ATGEN (F. Brunner and T. Nürnberger).

Elf26

Seedling data for elf26 (1 μM, 60 min) obtained in *A. thaliana* Landsberg ecotype were downloaded from ArrayExpress, European Bioinformatics Institute (EBI): E-MEXP 547, H elf wt 60 min (2 arrays) (G. Kunz).

Chitin

Leaf data for chitin (1 μM, 30 min) were downloaded from Gene Expression Omnibus, http://www.ncbi.nlm.nih.gov/projects/geo/, at NCBI, dataset record

GDS1531. Crab-shell chitin: GSM48125, GSM48126, GSM48127; control: GSM48128, GSM48129, GSM48130 (K. Ramonell, GSE2538 Chitin Oligomer Experiment).

Harpin

Leaf data for harpin (4 h) were downloaded from AtGenExpress at TAIR website, TAIR accession: ExpressionSet:1008080727. HrpZ, 4 h: B11-ATGEN, B25 ATGEN, B39-ATGEN (AtGenExpress, F. Brunner and T. Nürnberger).

NPP1

Leaf data for NPP1 (4 h) were downloaded from AtGenExpress at TAIR website, TAIR accession: ExpressionSet:1008080727. NPP1, 4 h: B12-ATGEN, B26-ATGEN, B40-ATGEN (AtGenExpress, F. Brunner and T. Nürnberger). For these arrays, the controls used were 4 h: B10-ATGEN, B24-ATGEN, B38-ATGEN.

LPS

Leaf data for LPS (4 h) were downloaded from AtGenExpress at TAIR website, TAIR accession: ExpressionSet:1008080727. LPS 4 h: B14-ATGEN, B28-ATGEN, B42-ATGEN (AtGenExpress, F. Brunner and T. Nürnberger).

PGN

Leaf data for PGN (4 h) were obtained from A. Gust and T. Nürnberger in the form of Affymetrix .CEL files that were used for data analysis.

ABA

Data for ABA treatment (10 μM, 60 min) in seedlings were downloaded from AtGenExpress at TAIR website, TAIR accession: ExpressionSet: 1007964750. ABA 1 h: RIKEN-GODA13ARIKEN-GODA13B, RIKEN-GODA1A, RIKEN-GODA1B (AtGenExpress, H. Goda, S. Yoshida, Y. Shimada).

P.s. phaseolicola

Data for *P.s. phaseolicola* infection (6 h) were downloaded from AtGenExpress at TAIR website, TAIR accession: ExpressionSet:1007966202. *Pseudomonas syringae pv. phaseolicola*, 6 h: A45-ATGEN-31-1_6hr_PSPH, A46-ATGEN-31-2_6hr_PSPH, A48-ATGEN-31-4_6hr_PSPH (AtGenExpress, B. Kemmerling and T. Nürnberger).

B. cinerea

Data for *B. cinerea* infection (18 h) were downloaded from AtGenExpress at TAIR website, TAIR accession: ExpressionSet:1007967417. *Botrytis cinerea*, 18 h: BC181-1, BC181-2, BC181-3 (AtGenExpress, C. Denoux, F. Ausubel, J. Dewdney, S. Ferrari).

P. infestans

Data for *P infestans* infection (12 h) were downloaded from AtGenExpress at TAIR website, TAIR accession: ExpressionSet:1007966021. *Phytophthora infestans*, 12 h: C13-ATGEN-1-PI-12, C14-ATGEN-2-PI-12, C15-ATGEN-3-PI-12 (AtGenExpress, D. Scheel, F. Brunner, L. Westphal).

SUPPLEMENTARY REFERENCES

1. Zimmermann, P., Hennig, L. & Gruissem, W. Gene-expression analysis and network discovery using Genevestigator. *Trends Plant Sci.* **10**, 407-409 (2005).
2. Harper, J. F. & Harmon, A. Plants, symbiosis and parasites: a calcium signalling connection. *Nat. Rev. Mol. Cell Biol.* **6**, 555-66 (2005).
3. Cheng, S. H., Willmann, M. R., Chen, H. C. & Sheen, J. Calcium signaling through protein kinases. The *Arabidopsis* calcium-dependent protein kinase gene family. *Plant Physiol.* **129**, 469-485 (2002).
4. Sheen, J. Ca^{2+}-dependent protein kinases and stress signal transduction in plants. *Science* **274**, 1900-1902 (1996).
5. Burch-Smith, T. M., Schiff, M., Liu, Y. & Dinesh-Kumar, S. P. Efficient virus-induced gene silencing in *Arabidopsis*. *Plant Physiol.* **142**, 21-27 (2006).
6. Baena-Gonzalez, E., Rolland, F., Thevelein, J. M. & Sheen, J. A central integrator of transcription networks in plant stress and energy signalling. *Nature* **448**, 938-942 (2007).
7. Asai, T. et al. MAP kinase signalling cascade in *Arabidopsis* innate immunity. *Nature* **415**, 977-983 (2002).
8. He, P. et al. Specific bacterial suppressors of MAMP signaling upstream of MAPKKK in Arabidopsis innate immunity. *Cell* **125**, 563-575 (2006).

9. Shan, L. et al. Bacterial effectors target the common signaling partner BAK1 to disrupt multiple MAMP receptor-signaling complexes and impede plant immunity. *Cell Host Microbe* **4**, 17-27 (2008).

10. Yoo, S. D., Cho, Y. H. & Sheen, J. Arabidopsis mesophyll protoplasts: a versatile cell system for transient gene expression analysis. *Nat. Protoc.* **2**, 1565-1572 (2007).

11. Schreiber, K., Ckurshumova, W., Peek, J. & Desveaux, D. A high-throughput chemical screen for resistance to Pseudomonas syringae in Arabidopsis. *Plant J.* **54**, 522-531 (2008).

12. Kauffmann, A., Gentleman, R. & Huber, W. arrayQualityMetrics--a bioconductor package for quality assessment of microarray data. *Bioinformatics* **25**, 415-416 (2009).

13. Suarez-Farinas, M., Pellegrino, M., Wittkowski, K. M. & Magnasco, M. O. Harshlight: a "corrective make-up" program for microarray chips. R package version 1.12.0. (2007). http://asterion.rockefeller.edu/Harshlight/

14. Reimers, M. & Weinstein, J. N. Quality assessment of microarrays: visualization of spatial artifacts and quantitation of regional biases. *BMC Bioinformatics* **6**, 166 (2005).

15. Choe, S. E., Boutros, M., Michelson, A. M., Church, G. M. & Halfon, M. S. Preferred analysis methods for Affymetrix GeneChips revealed by a wholly defined control dataset. *Genome Biol.* **6**, R16 (2005).

16. Cheng, C. & Pounds, S. False discovery rate paradigms for statistical analyses of microarray gene expression data. *Bioinformation* **1**, 436-446 (2007).

17. Murie, C., Woody, O., Lee, A. Y. & Nadon, R. Comparison of small n statistical tests of differential expression applied to microarrays. *BMC Bioinformatics* **10**, 45 (2009).

18. Blazejczyk, M., Miron, M. & Nadon, R. FlexArray: a statistical data analysis software for gene expression microarrays (Genome Quebec, Montreal, Canada, 2007).
URL http://genomequebec.mcgill.ca/FlexArray

19. Irizarry, R. A. et al. Summaries of Affymetrix GeneChip probe level data. *Nucleic Acids Res.* **31**, e15 (2003).

20. Irizarry, R. A. et al. Exploration, normalization, and summaries of high density oligonucleotide array probe level data. *Biostatistics* **4**, 249-264 (2003).

21. Li, C. & Hung Wong, W. Model-based analysis of oligonucleotide arrays: model validation, design issues and standard error application. *Genome Biol.* **2**, 0032 (2001).

22. Hubbell, E., Liu, W. M. & Mei, R. Robust estimators for expression analysis. *Bioinformatics* **18**, 1585-1592 (2002).

23. Tusher, V. G., Tibshirani, R. & Chu, G. Significance analysis of microarrays applied to the ionizing radiation response. *Proc. Natl. Acad. Sci. U S A* **98**, 5116-5121 (2001).

24. Baldi, P. & Long, A. D. A Bayesian framework for the analysis of microarray expression data: regularized t -test and statistical inferences of gene changes. *Bioinformatics* **17**, 509-519 (2001).

25. Affymetrix: Microarray suite user guide. Affymetrix 2001, version 5: http://www.affymetrix.com/support/technical/manuals.affx

26. Thimm, O. et al. MAPMAN: a user-driven tool to display genomics data sets onto diagrams of metabolic pathways and other biological processes. *Plant J.* **37**, 914-939 (2004).

27. de Hoon, M. J., Imoto, S., Nolan, J. & Miyano, S. Open source clustering software. *Bioinformatics* **20**, 1453-1454 (2004).

28. Saldanha, A. J. Java Treeview--extensible visualization of microarray data. *Bioinformatics* **20**, 3246-3248 (2004).

29. Zipfel, C. et al. Perception of the bacterial PAMP EF-Tu by the receptor EFR restricts Agrobacterium-mediated transformation. *Cell* **125**, 749-760 (2006).

30. Ramonell, K. et al. Loss-of-function mutations in chitin responsive genes show increased susceptibility to the powdery mildew pathogen Erysiphe cichoracearum. *Plant Physiol.* **138**, 1027-1036 (2005).

31. Lee, J., Klessig, D. F. & Nurnberger, T. A harpin binding site in tobacco plasma membranes mediates activation of the pathogenesis-related gene HIN1 independent of extracellular calcium but dependent on mitogen-activated protein kinase activity. *Plant Cell* **13**, 1079-1093 (2001).

32. Fellbrich, G. et al. NPP1, a Phytophthora-associated trigger of plant defense in parsley and Arabidopsis. *Plant J.* **32**, 375-390 (2002).

33. Qutob, D. et al. Phytotoxicity and innate immune responses induced by Nep1-like proteins. *Plant Cell* **18**, 3721-3744 (2006).

34. Zeidler, D. et al. Innate immunity in Arabidopsis thaliana: lipopolysaccharides activate nitric oxide synthase (NOS) and induce defense genes. *Proc. Natl. Acad. Sci. U S A* **101**, 15811-15816 (2004).

35. Gust, A. A. et al. Bacteria-derived peptidoglycans constitute pathogen-associated molecular patterns triggering innate immunity in Arabidopsis. *J. Biol. Chem.* **282**, 32338-32348 (2007).

36. Ferrari, S. et al. Resistance to Botrytis cinerea induced in Arabidopsis by elicitors is independent of salicylic acid, ethylene, or jasmonate signaling but requires PHYTOALEXIN DEFICIENT3. *Plant Physiol.* **144**, 367-379 (2007).